JACS
JOURNAL OF THE AMERICAN CHEMICAL SOCIETY
pubs.acs.org/JACS

Article

Controlled Surface Modification of Cobalt Phosphide with Sulfur Tunes Hydrogenation Catalysis

Nina A. Arnosti, Vanessa Wyss, and Murielle F. Delley*

Cite This: J. Am. Chem. Soc. 2023, 145, 23556−23567

Read Online

ACCESS | Metrics & More | Article Recommendations | Supporting Information

ABSTRACT: Transition metal phosphides have shown promise as catalysts for water splitting and hydrotreating, especially when a small amount of sulfur is incorporated into the phosphides. However, the effect of sulfur on catalysis is not well understood. In part, this is because conventional preparation methods of sulfur-doped transition metal phosphides lead to sulfur both inside and at the surface of the material. Here, we present an alternative method of modifying cobalt phosphide (**CoP**) with sulfur using molecular S-transfer reagents, namely, phosphine sulfides (SPR_3). SPR_3 added sulfur to the surface of **CoP** and using a series of SPR_3 reagents having different P═S bond strengths enabled control over the amount and type of sulfur transferred. Our results show that there is a distribution of different sulfur sites possible on the **CoP** surface with S-binding strengths in the range of 69 to 84 kcal/mol. This provides fundamental information on how sulfur binds to an amorphous **CoP** surface and provides a basis to assess how number and type of sulfur on **CoP** influences catalysis. For the catalytic hydrogenation of cinnamaldehyde, intermediate amounts of sulfur with intermediate binding strengths at the surface of **CoP** were optimal. With some but not too much sulfur, **CoP** exhibited a higher hydrogenation productivity and a decreased formation of secondary reaction products. Our work provides important insight into the S-effect on the catalysis by transition metal phosphides and opens new avenues for catalyst design.

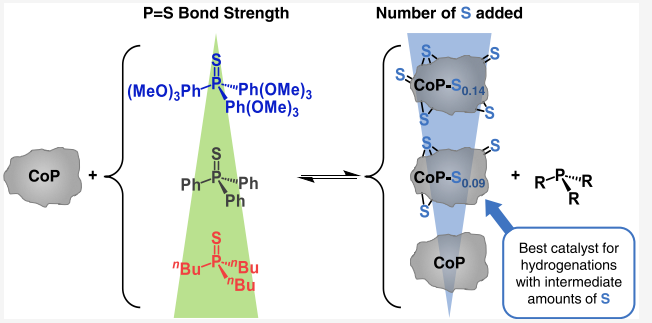

INTRODUCTION

Due to their promising catalytic properties for water splitting and hydrodesulfurization, transition metal phosphides are being discussed as potential earth-abundant replacements for the conventional noble-metal-based catalysts.[1−6] Key to an actual implementation of transition metal phosphides in catalytic applications is to optimize their properties for catalysis. Two very successful optimization approaches involve the doping of transition metal phosphides with foreign elements or the direct preparation of composite materials containing multiple elements.[3,7,8] For instance, transition metal phosphides that incorporate a small amount of sulfur have shown higher electrocatalytic activity and stability in the hydrogen evolution reaction (HER) compared to the pristine phosphides.[9−17] A similar sulfur effect has been observed in hydrodesulfurization applications: During hydrodesulfurization the transition metal phosphides are *in situ* sulfided by H_2S and form phosphosulfides at the surface.[18−21] It has been proposed that the phosphosulfide surfaces are the catalytically relevant surfaces and that sulfur enhances the catalytic activity as part of the catalytically active sites.[22−28] The promoting effect of sulfur on activity or selectivity has also been noted for other heterogeneous catalysts.[29] These literature reports highlight the potential of using sulfur to modify transition metal phosphides for improved catalytic properties.

The promoting effect of sulfur on the catalysis of transition metal phosphides has variously been attributed to the formation of new or modified active sites that incorporate S at the surface,[9,11,18−20,22,24] optimized binding energies of hydrogen at the surface,[10,12,13,15−17,30] improved electronic properties that facilitate charge transfer,[12−15,17,30] increased surface areas,[12,14] or higher number of active sites.[13,14] However, some studies suggest that sulfur can also act as a poison on transition metal phosphide hydrodesulfurization catalysts.[31−33] Overall, the sulfur effect in (electro)catalysis is not well understood. In part, this is likely because conventional approaches to prepare S-doped transition metal phosphides or metal,P,S-composite materials do not target the preparation of specific S-sites. The synthesis of such materials typically includes solid−gas reactions of material precursors with *in situ* formed $PH_{3(g)}$ and $H_2S_{(g)}$ or, alternatively, the mixing and heating of metal-, P-, and S-precursors at elevated temperatures.[5,9,10,12,13,17,30,34−36] By these methods, sulfur can be

Received: July 10, 2023
Revised: September 19, 2023
Accepted: October 9, 2023
Published: October 24, 2023

incorporated with a wide range of chemical environments and both inside the material and on the surface. It is therefore challenging to experimentally distinguish between bulk and surface effects of sulfur in catalysis or to attribute any observed sulfur effect to a specific active site. To understand how sulfur modifies the properties and reactivity of transition metal phosphides, computational approaches have hence often been used.[10,11,13−16,19,30,36] However, such theoretical approaches usually need to be performed on crystalline facet models, which have limited relevance with respect to the typically amorphous surfaces of heterogeneous catalysts under experimental conditions.[37−40]

Herein, we address these challenges by pursuing an experimental strategy to access thermochemical information about different S-sites on a transition metal phosphide and to probe their effect on catalysis. We report a more controlled approach of modifying cobalt phosphide (**CoP**) with sulfur that includes the reaction of **CoP** with different phosphine sulfides (SPR_3). Phosphine chalcogenide reagents have previously been used for the synthesis and transformation of metal chalcogenide nanoparticles,[41−47] and SPR_3 are well-documented S-transfer reagents in molecular coordination chemistry.[48−52] We show that this S-transfer ability of the SPR_3 reagents enabled the addition of S to **CoP** at the surface and with varied number and type of S. Furthermore, we employed equilibration reactions of **CoP** with different SPR_3 to provide new insight into the thermochemistry of sulfur binding to **CoP**. We tested the bare and S-modified **CoP** as catalysts for the hydrogenation of cinnamaldehyde and showed that varied number and binding strength of S on the **CoP** surface diversely influenced the productivity, activity, and selectivity of the reaction.

RESULTS

Synthesis and Characterization of CoP. **CoP** was synthesized via a solid-state transformation from cobalt oxide and sodium hypophosphite as the phosphorus source in an argon flow at 300 °C, as described previously.[53,54] The as-prepared **CoP-ox** was treated with diluted sulfuric acid to remove the oxidized surface layer and then handled under strictly air- and moisture-free conditions.[54] UV/vis spectroscopic analysis of the washing solution showed the presence of $Co^{2+}_{(aq)}$, suggesting that the acid washing procedure removed 0.002 mol of Co from the surface per gram of as-prepared **CoP-ox**. This corresponds to a removal of roughly the top four atomic layers based on our estimate of exposed surface atoms (see SI and ref 54). Co 2p and P 2p X-ray photoelectron spectra (XPS) of the acid-washed **CoP** showed no or decreased signals attributable to **Co**-O_x and **P**-O_x and signals characteristic for **Co**-P and **P**-Co, respectively, indicating the removal of most of the oxidized surface and exposure of a bare cobalt phosphide surface. The acid-washed **CoP** material is a black powder consisting of particles with sizes ranging from roughly 10 to 300 μm, as shown by scanning electron microscopy (SEM). Combined analyses by powder X-ray diffraction (pXRD), energy-dispersive X-ray spectroscopy (EDX), and elemental analysis showed that **CoP** is largely amorphous with a 1:1 Co:P ratio. N_2 adsorption measurements suggested that **CoP** has a Brunauer−Emmett−Teller (BET) surface area of ∼38 m^2/g. From the measured surface area and predominant phase and by assuming spherical particles of identical size we estimate that ∼5% of all "CoP" units in the material are exposed on the surface. See SI for further details on material synthesis, characterization, and the estimation of surface "CoP" units.

Controlled Sulfur Transfer to CoP. To modify **CoP** with sulfur, we probed the use of molecular sulfur-transfer reagents. For this, **CoP** was reacted with three different phosphine sulfide reagents, SPR_3, having different P═S bond dissociation free energies (BDFEs): tri-*n*-butyl phosphine sulfide (SP^nBu_3, P═S BDFE = 84 kcal/mol), triphenyl phosphine sulfide ($SPPh_3$, P═S BDFE = 76 kcal/mol), and tris(2,4,6-trimethoxyphenyl)phosphine sulfide (TriMePS, P═S BDFE = 69 kcal/mol). The BDFEs of the P═S bond of the different SPR_3 reagents were estimated from their reported bond dissociation enthalpies (BDEs),[49,55−60] solvation free energies,[55] and standard entropies,[55,61] by making a few necessary assumptions that are reasonable first approximations based on prior reports (e.g., similar standard entropies $S°(PR_3) \approx S°(SPR_3)$ and similar free energies of solvation $\Delta G°solv(R_3P) \approx \Delta G°solv(R_3P{=}S)$)[55] and by comparison to P═S bond strengths calculated by density functional theory (DFT) methods.[56] See the SI for more details. There is some uncertainty in the BDFEs derived by this method due to the applied assumptions, but the obtained BDFE estimates are sufficiently accurate to show the trends of interest herein.

The S-transfer reactions between **CoP** and the different SPR_3 reagents were conducted at 80 °C in J-Young NMR tubes under inert conditions with a large excess of SPR_3 (Figure 1a). We monitored the reaction progress by ^1H and $^{31}P\{^1H\}$ NMR spectroscopy. PR_3 formation was observed when using $SPPh_3$ or TriMePS as S-transfer reagents but not with SP^nBu_3 (Figure 1b). This suggests that the former two SPR_3 reagents with lower P═S BDFE can add S to **CoP**, giving **CoP-S**$_x$, and SP^nBu_3, having the highest P═S BDFE, cannot add S to **CoP**. The reaction of **CoP** with $SPPh_3$ or TriMePS formed the corresponding PR_3 as the sole product in solution. Only at long reaction times (after 450 or 70 h for $SPPh_3$ or TriMePS, respectively) were trace amounts of side-products observed, such as OPR_3 or other unidentified side-products likely from TriMePS decomposition. Similar S-transfer reactions of **CoP** with the different SPR_3 were also tested on a larger scale of 100−200 mg of **CoP** to enable postreaction analysis of the **CoP-S**$_x$. NMR analysis of the solution from these larger scale experiments with $SPPh_3$ or TriMePS showed the corresponding PR_3 product, which suggested a successful S-transfer, similar to the NMR-scale reactions. The obtained **CoP-S**$_x$ was analyzed by XPS, elemental analysis, and EDX. These analyses showed that the **CoP-S**$_x$ obtained from the reaction of **CoP** with either $SPPh_3$ or TriMePS contained sulfur. A quantitative analysis of S-content at the surface is difficult with the XPS data quality in hand due to the low signal-to-noise ratio of the S 2p signal. However, the XPS data account for the S-content detected by bulk techniques and are hence consistent with all S being located at the **CoP** surface (Figure 1c and the SI). Sulfur delivery to the surface is also consistent with the pXRD analysis of **CoP-S**$_x$ showing an amorphous CoP pattern similar to **CoP** and without changes expected for significant S in the bulk structure (SI).[10,16,35,62] Furthermore, sulfur delivery to the surface is in line with the employed method of S-modification involving molecular SPR_3 reagents that are too large to go inside the solid, nonporous **CoP** material. Combined, all data showed a successful S-transfer with $SPPh_3$ and TriMePS to the surface of **CoP**.

https://doi.org/10.1021/jacs.3c07312
J. Am. Chem. Soc. 2023, 145, 23556−23567

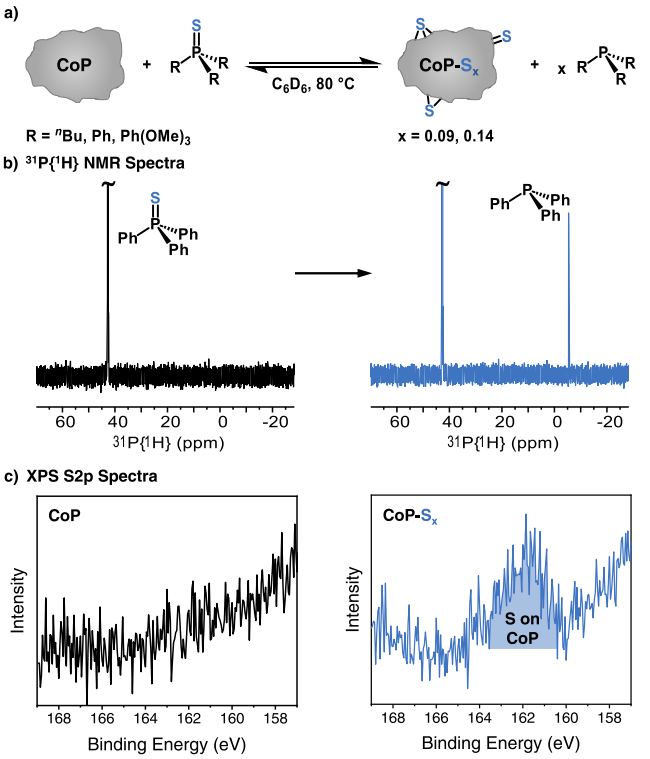

Figure 1. (a) Reaction of **CoP** with an excess of different phosphine sulfide reagents SPR_3 (R = ^{n}Bu, Ph, or Ph(OMe)$_3$ (TriMeP)). Two of the SPR_3 (R = Ph or Ph(OMe)$_3$ (TriMeP)) added sulfur to **CoP** and formed **CoP-S$_x$** and PR_3. (b) $^{31}P\{^1H\}$ NMR spectra before (black, left) and after reaction (blue, right) of **CoP** with $SPPh_3$ at 80 °C for 500 h showing signals corresponding to the reagent $SPPh_3$ at 43 ppm and the formed PPh_3 at −5 ppm. (c) X-ray photoelectron spectroscopy (XPS) S 2p spectra of the bare **CoP** (black, left) and **CoP-S$_{0.09}$** (blue, right) showing that S has been added to the surface of **CoP** by reaction with $SPPh_3$. Similar NMR and XPS data were obtained for TriMePS, while the absence of a P^{n}Bu$_3$ NMR signal in the case of SP^{n}Bu$_3$ showed that SP^{n}Bu$_3$ did not add S to **CoP** (see the SI).

To learn more about the S-sites generated on **CoP-S$_x$** by the S-transfer reactions between **CoP** and SPR_3, we let the reaction mixtures of **CoP** and each SPR_3 reagent equilibrate until no further PR_3 product formation was observed (after > ∼250 h). We quantified the amount of PR_3 formed by ^1H and $^{31}P\{^1H\}$ NMR analysis after equilibration and used this analysis to infer the number of S atoms transferred to **CoP** normalized to the number of "CoP" units exposed at the surface (Figure 2). The analysis from eight and five independent replicate measurements using two different batches of **CoP** suggested that 0.09(1) and 0.14(1) S per surface "CoP" could be transferred from $SPPh_3$ and TriMePS, respectively. Herein, we denote the obtained S-modified **CoP-S$_x$** with **CoP-S$_{0.09}$** and **CoP-S$_{0.14}$**, respectively, where the nomenclature refers to their stoichiometries at the surface. For **CoP** batches that have been prepared under slightly different conditions (e.g., with a different acid-washing time to remove the oxidized surface or a different drying time) the absolute numbers of transferred S per surface "CoP" can vary by up to a factor of two, probably due to variations in surface area of the **CoP** or surface coverage by water (see the SI). However, for **CoP** batches prepared under carefully controlled and identical conditions we obtained the number of S per surface "CoP" (0.09 and 0.14) with only a ∼10% uncertainty, which is surprisingly small given the heterogeneous nature and large particle size distribution of the **CoP** material. The NMR data from the S-transfer reactions suggest that TriMePS can add ∼1.5 times as much S to **CoP** as $SPPh_3$. This is consistent with the sulfur quantification results from XPS, elemental analysis, and EDX, each showing that the sulfur content on **CoP-S$_{0.14}$** from TriMePS is larger than that on **CoP-S$_{0.09}$** from $SPPh_3$ (see the SI). Together, the data consistently show that TriMePS can add more S to the surface of **CoP** than $SPPh_3$.

The above equilibration data clearly show that different SPR_3 reagents added different amounts of S to **CoP** per surface "CoP": SP^{n}Bu$_3$ added none, $SPPh_3$ added an intermediate amount, and TriMePS added roughly 1.5 as much S to **CoP** as $SPPh_3$. There are several possible explanations for these findings. One possibility is that the SPR_3 reagents add S to different sites on **CoP** according to their P═S BDFEs in

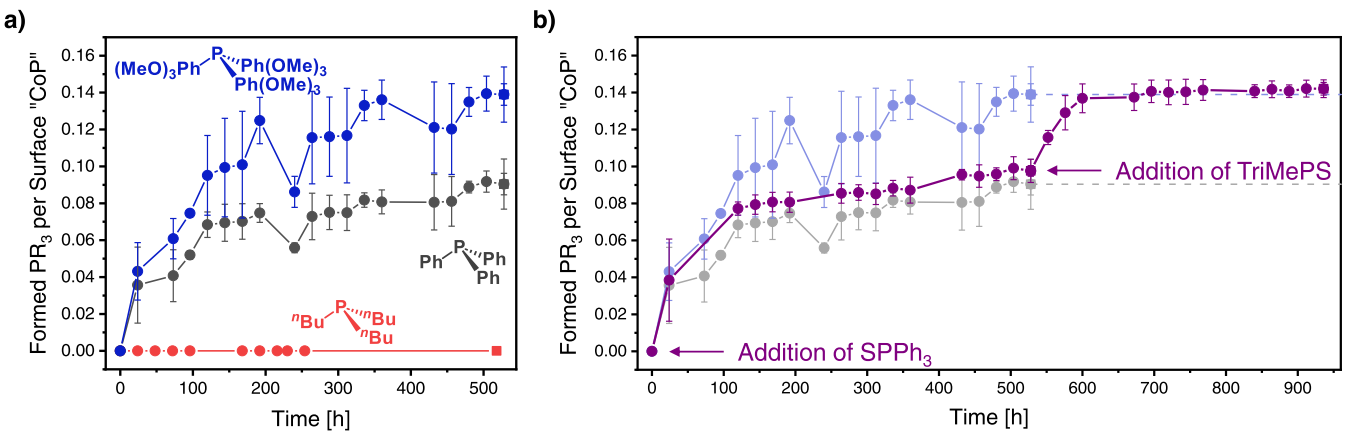

Figure 2. PR_3 formed per "CoP" unit on the surface vs time as monitored by $^{31}P\{^1H\}$ NMR for (a) S-transfer reactions between **CoP** and SP^{n}Bu$_3$ (red), $SPPh_3$ (gray), or TriMePS (blue, SP(Ph(OMe)$_3$)$_3$) and (b) a comparison of these data with the PR_3 formation from a sequential S-addition experiment of using first $SPPh_3$ at 0 h and then TriMePS at 530 h (purple). PR_3 quantification was performed by taking an additional $^{31}P\{^1H\}$ NMR spectrum using a longer relaxation delay d1 = 20 s after equilibration at the conclusion of each experiment (squares) and scaling all prior measurements (dots) according to the final measurement (see the SI for further details). Error bars are derived from three or more replicate experiments.

https://doi.org/10.1021/jacs.3c07312
J. Am. Chem. Soc. 2023, 145, 23556−23567

solution. For instance, SP^{n}Bu$_3$, having the strongest P═S interaction, was not able to transfer S to any sites on **CoP**. SPPh$_3$, with an intermediately strong P═S bond, transferred S to some sites on **CoP**, while TriMePS, with the weakest P═S bond, transferred S to the most sites on **CoP** among the three SPR$_3$. However, there may also be other contributors to the reaction free energy that influence the observed equilibria, such as substrate or product binding to the **CoP** surface. In fact, some formed PR$_3$ seemed to bind strongly to **CoP-S$_x$**: After washing the **CoP-S$_x$** no more SPR$_3$ or PR$_3$ could be detected by NMR in the washing solution. However, we did observe 0.002−0.003 equiv of PR$_3$ per surface "CoP" in the solution by ^{31}P{^{1}H} NMR when heating the thoroughly washed **CoP-S$_x$** to 80 °C in d_6-benzene, and 0.01−0.014 PR$_3$ per surface "CoP" when heating **CoP-S$_x$** in the presence of P^{n}Bu$_3$. This suggests that there is strongly surface-bound PR$_3$ that can desorb from the surface at 80 °C and especially by exchange with P^{n}Bu$_3$. In light of these data and the possible influence of surface binding, we probed whether the observed less extensive S-transfer with SP^{n}Bu$_3$ or SPPh$_3$ compared to TriMePS is because the corresponding SPR$_3$ or PR$_3$ blocks the surface, thereby hindering further S-transfer or if it can be attributed to their respective P═S bond strengths. For this, we reacted **CoP** first with SPPh$_3$, washed the obtained **CoP-S$_{0.09}$**, and then reacted **CoP-S$_{0.09}$** with TriMePS in a second step. Figure 2b shows the PR$_3$ product quantification by NMR of this sequential experiment and compares it to the direct S-transfer experiment with TriMePS only. This analysis suggested a similar total of 0.14 ± 0.02 or 0.142 ± 0.003 PR$_3$ formed (or, S transferred to **CoP**) per surface "CoP" for a direct reaction with TriMePS or a sequential experiment with SPPh$_3$ then TriMePS, respectively. Hence, after the S-transfer to **CoP** from SPPh$_3$ more S can still be added to **CoP-S$_{0.09}$** using TriMePS, and the number of S transferred is equivalent to what is obtained when reacting TriMePS directly with the bare **CoP**. This suggests that the **CoP** surface is not significantly blocked for further transfer after reaction with SPPh$_3$. Therefore, the higher amount of S added to **CoP** from TriMePS than from SPPh$_3$ can probably be mainly attributed to their different P═S bond strengths allowing a S-addition to different sites on **CoP**.

Reversibility of the S-Transfer Reactions. We probed the reversibility of the S-transfers to **CoP** by reacting a large excess of P^{n}Bu$_3$ with **CoP-S$_x$** (obtained from reaction of **CoP** with SPPh$_3$ or TriMePS), yielding **CoP-S$_{x-y}$** (Figure 3). SP^{n}Bu$_3$ has a higher P═S BDFE than SPPh$_3$ or TriMePS, and P^{n}Bu$_3$ could hence provide enough driving force to remove S from **CoP-S$_x$**. These S-removal reactions were conducted under similar conditions to the S-transfer reactions to **CoP** described above, i.e., at 80 °C under an inert atmosphere with monitoring the reaction solution by ^{31}P{^{1}H} NMR spectroscopy and with analysis of the formed **CoP-S$_{x-y}$** by XPS (Figure 3b,c). NMR signals attributed to the formation of SP^{n}Bu$_3$ were observed on a time scale of 24 h until ∼400 h.

The reaction of P^{n}Bu$_3$ with **CoP-S$_{0.09}$** formed 0.042(8) equiv of SP^{n}Bu$_3$ per surface "CoP". This suggests that ∼45% of the S originally transferred to **CoP** with SPPh$_3$ are removed from the **CoP-S$_{0.09}$** surface. The reaction of P^{n}Bu$_3$ with **CoP-S$_{0.14}$** formed 0.11(1) equiv of SP^{n}Bu$_3$ per surface "CoP", corresponding to ∼75% of the S originally transferred to **CoP** with TriMePS (Figure 4). In both cases, some S seems to remain on **CoP-S$_{x-y}$** (in roughly similar amounts on the order of ∼0.03−0.05 equiv of S per surface "CoP"), and this S cannot be removed by reaction with P^{n}Bu$_3$. Figure 4a shows

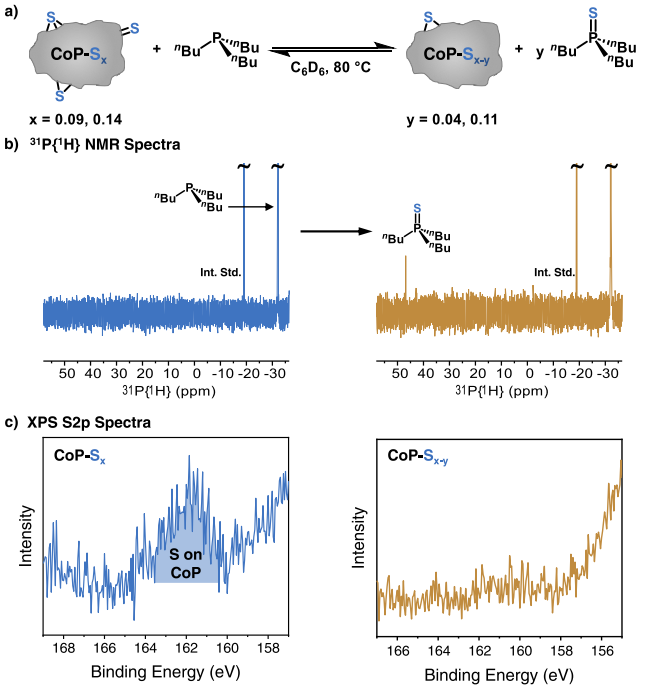

Figure 3. (a) Reaction with P^{n}Bu$_3$ removed sulfur from **CoP-S$_x$** and formed SP^{n}Bu$_3$ and **CoP-S$_{x-y}$**. (b) ^{31}P{^{1}H} NMR spectrum before reaction of **CoP-S$_{0.09}$** with P^{n}Bu$_3$ (blue, left) showing P^{n}Bu$_3$ at −32 ppm (and the internal standard OP(OPh)$_3$ at −17 ppm), and ^{31}P{^{1}H} NMR spectrum after reaction of **CoP-S$_{0.09}$** with P^{n}Bu$_3$ at 80 °C for 580 h (yellow, right) showing the formation of SP^{n}Bu$_3$. (c) XPS S 2p spectra of **CoP-S$_{0.09}$** (blue, left) and **CoP-S$_{0.09-0.04}$** (yellow, right) showing the presence and absence of a S peak, respectively, indicating that S has been removed from the surface of **CoP-S$_{0.09}$** through the reaction with P^{n}Bu$_3$.

the amount of S on **CoP-S$_{x-y}$** as a function of the reaction time, and Figure 4b shows an overview of the S originally present on **CoP-S$_x$** and the S left on **CoP-S$_{x-y}$**. Analysis of **CoP-S$_{x-y}$** by XPS, elemental analysis, and EDX showed a decreased S content compared to the original **CoP-S$_x$**, which is consistent with the removal of some of the S but not all (see the SI). A more quantitative analysis of the S remaining on **CoP-S$_{x-y}$** is difficult by these methods due to the small amount of S on the materials. However, in the case of the **CoP-S$_{x-y}$** originally stemming from a S-transfer to **CoP** with TriMePS the S detected at the surface by XPS does not seem to quantitatively account for the S detected in bulk by elemental analysis of the **CoP-S$_{x-y}$** (see the SI). This could be a consequence of the uncertainty associated with the low signal-to-noise ratio in the XPS spectrum, chemical changes at the surface, or alternatively because some S is inside the **CoP-S$_{x-y}$** particles. The former two are more likely since XPS analysis of the **CoP-S$_{x-y}$** showed that the cobalt phosphide surface was partially oxidized after reaction with P^{n}Bu$_3$ and that there was residual S-content at the surface (see the SI). Surface oxidation is also consistent with the OP^{n}Bu$_3$ observed by ^{31}P{^{1}H} NMR that was formed in roughly a similar amount as the formed SP^{n}Bu$_3$ in the reaction of P^{n}Bu$_3$ with **CoP-S$_x$** (see the SI). OP^{n}Bu$_3$ could stem from the reaction of P^{n}Bu$_3$ with trace amounts of O$_2$ in the reaction mixture or with residual oxygen on the **CoP-S$_x$** surface. All data are hence consistent with the partial removal of S from **CoP-S$_x$** and surface oxidation of **CoP-S$_{x-y}$** showing that the S-transfers to **CoP** are reversible to some extent.

https://doi.org/10.1021/jacs.3c07312
J. Am. Chem. Soc. 2023, 145, 23556−23567

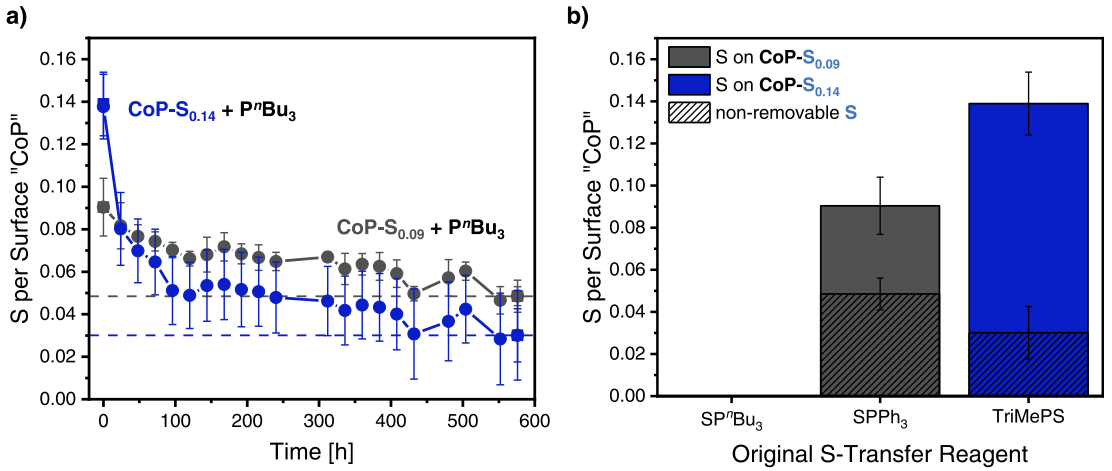

Figure 4. (a) Sulfur on **CoP-S$_{x\text{-}y}$** per "CoP" unit vs time based on the formation of SP^{n}Bu$_3$ during the reaction of P^{n}Bu$_3$ with either **CoP-S$_{0.14}$** (blue) or **CoP-S$_{0.09}$** (gray) as monitored by ^{31}P{^{1}H} NMR spectroscopy. SP^{n}Bu$_3$ quantification was performed by taking an additional ^{31}P{^{1}H} NMR spectrum using a longer relaxation delay d1 = 20 s at the conclusion of an experiment (squares) and scaling all prior measurements (dots) according to the final measurement (see the SI for details). (b) Overview of the amount of sulfur per surface "CoP" unit on **CoP-S$_x$** from S-transfer to **CoP** using SP^{n}Bu$_3$ (none), SPPh$_3$ (gray), or TriMePS (blue), and the amount of S that cannot be removed by reaction with P^{n}Bu$_3$ (shaded areas). Error bars are derived from five or more replicate experiments.

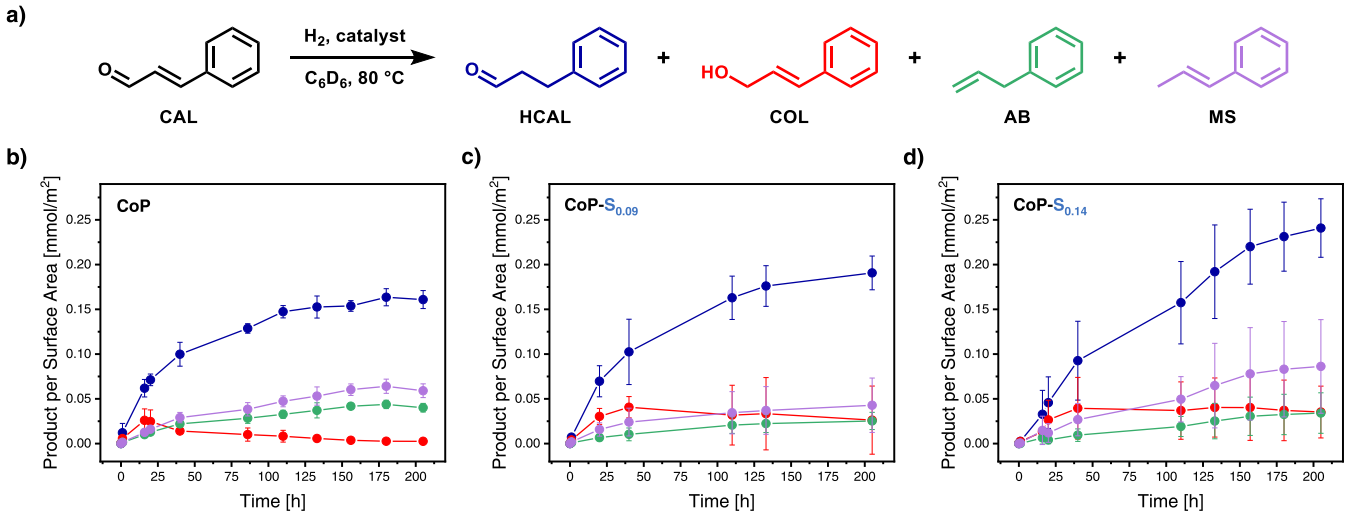

Figure 5. (a) Hydrogenation of cinnamaldehyde (CAL) using **CoP**, **CoP-S$_{0.09}$**, or **CoP-S$_{0.14}$** as catalysts. The corresponding product formation as a function of time is shown in (b), (c), and (d), respectively.

Catalytic Performance in Hydrogenation Reactions. In view of prior reports suggesting a beneficial effect of sulfur in transition metal phosphides for the (electro-)catalysis of HER and hydrotreating,[9−21] and the known activity of bare transition metal phosphides in the hydrogenation of α,β-unsaturated aldehydes,[63−66] we tested the bare **CoP** and the two S-modified **CoP-S$_{0.09}$** and **CoP-S$_{0.14}$** as catalysts for the hydrogenation of cinnamaldehyde (Figure 5a). The reactions were performed in C_6D_6 at 80 °C with ∼2 bar of H_2 in J-Young NMR tubes and monitored by ^{1}H NMR spectroscopy. **CoP**, **CoP-S$_{0.09}$**, and **CoP-S$_{0.14}$** were all active catalysts for the hydrogenation of cinnamaldehyde and formed hydrocinnamaldehyde (HCAL) and cinnamyl alcohol (COL), and also allylbenzene (AB) and β-methylstyrene (MS), while no product formation was observed in the absence of a catalyst. Figure 5b−d compare the product formation normalized with surface area versus time in the presence of **CoP**, **CoP-S$_{0.09}$**, or **CoP-S$_{0.14}$**, each averaged from four to six replicate measurements using multiple batches of **CoP** or **CoP-S$_x$** (see the SI for individual measurements). While the data are highly reproducible for **CoP**, there is more scatter in the data for **CoP-S$_x$**, especially for **CoP-S$_{0.14}$**. Nevertheless, we can identify some trends in the catalytic properties for hydrogenation as a function of the S-content in the **CoP** catalysts, as outlined below.

In the presence of the bare **CoP** similar amounts of HCAL and COL formed initially (after 1 h), consistent with a prior report.[63] HCAL is the main product observed under our conditions at longer reaction times. Products AB and MS were observed in steadily increasing but minor amounts. After increasing up to ∼20 h of reaction time, the amount of COL observed in the reaction mixture decreased. Hence, COL is likely a primary product as well as an intermediate, and AB and MS could be secondary products. After ∼100 h of reaction time, not much further product formation was observed under the NMR-scale batch conditions used herein.

To evaluate the catalytic performance of **CoP** as a function of the S content, we mainly consider the catalytic productivities

https://doi.org/10.1021/jacs.3c07312
J. Am. Chem. Soc. 2023, 145, 23556−23567

instead of intrinsic catalytic activities. Intrinsic activities should be evaluated by extrapolation to time 0, which is difficult with the data in hand. Qualitatively, the large amount of S on **CoP-$S_{0.14}$** seemed to decrease the intrinsic activity compared to that of **CoP** or **CoP-$S_{0.09}$**. Clearer trends were observed at longer reaction times in the catalytic productivity of **CoP** for hydrogenation as a function of the sulfur content. Larger amounts of hydrogenation products (HCAL and COL) were observed with the two **CoP-S_x** catalysts compared to the bare **CoP** after 200 h of reaction time (Figure 5 and the SI). However, at shorter reaction times of 20−40 h, **CoP-$S_{0.14}$** had formed less product than the bare **CoP**, and **CoP-$S_{0.09}$** had formed similar or perhaps slightly more product than the bare **CoP**. These data show that the sulfur content in **CoP** increased the overall productivity for cinnamaldehyde hydrogenation in the course of a reaction, but too much sulfur on **CoP** slowed product formation under our conditions at shorter reaction times.

The catalytic selectivity for cinnamaldehyde hydrogenation changed as a function of sulfur content in **CoP** (Figure 5). The major product was HCAL, while COL, AB, and MS were formed in relatively minor amounts in all cases. There were similar amounts of MS formed with **CoP** and **CoP-$S_{0.09}$**, but likely more MS formed at long reaction times with **CoP-$S_{0.14}$**. COL was initially formed in the presence of all materials in roughly similar amount to HCAL. However, with the bare **CoP** the amount of COL decreased again after ∼20 h, but with **CoP-$S_{0.09}$** or **CoP-$S_{0.14}$** the amount of COL was relatively constant after 20 h. There was less AB formed with **CoP-$S_{0.09}$** or **CoP-$S_{0.14}$** than with bare **CoP**. Overall, **CoP-$S_{0.09}$** and **CoP-$S_{0.14}$** both hence had higher selectivity for COL and formed less secondary AB than bare **CoP**, but **CoP-$S_{0.14}$** formed more secondary MS.

DISCUSSION

Bond Strength Distribution of Sulfur on Cobalt Phosphide. We have shown that the reaction of **CoP** with molecular S-transfer reagents, the phosphine sulfides SPR_3, modified **CoP** with sulfur and that this S-modification is partially reversible. By this method, the number of S transferred to **CoP** can directly be inferred from NMR data. Our approach enabled the addition of controlled amounts of S to **CoP** and a predominant location of S at the surface of **CoP**. This departs from previously reported methods for the preparation of S-doped transition metal phosphides that lead to S incorporation both at the surface and in bulk.[5,9,10,12,13,17,30,34−36]

Our results showed that different SPR_3 added different amounts of sulfur to **CoP** and that this correlated with the P═S bond strengths of the SPR_3 reagents: TriMePS with the weakest P═S bond added the most, $SPPh_3$ with an intermediately strong P═S bond added some, and SP^nBu_3 with the strongest P═S bond added no S to **CoP**. This shows that different sulfur sites are present on **CoP**. If there are no other significant contributors to the reaction free energy of the sulfur transfers, these data provide information about the sulfur binding strengths possible on **CoP**. This seems a good first approximation based on our results that PR_3 product binding to the surface did not appear to significantly influence the number of S transferred and based on the literature suggesting that, for example, the solvation free energies of SPR_3 and PR_3 are similar.[55] Our equilibration results of **CoP** with different SPR_3 hence show that *there is a distribution of different sites on CoP that can bind S with different bond strengths*. This is consistent with the previously reported distribution of sites on **CoP** for hydrogen binding[54,67] and with prior work suggesting that there are different kinds of surface sulfur species possible on transition metal phosphides.[19,21]

The S-transfer equilibria between **CoP** and different SPR_3 reagents hence provide a first approximation of the BDFE distribution of S binding to **CoP** (Figure 6). The observation

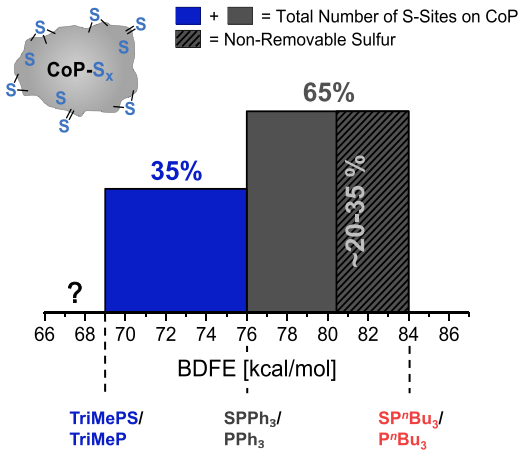

Figure 6. Schematic representation of the bond strength distribution for sulfur binding on **CoP** determined from equilibration of **CoP** with different SPR_3. The blue and gray areas represent the number of S-sites available on **CoP** for each BDFE range limited by the P═S bond strengths of the SPR_3 reagents used. The larger the area, the more sites available. The sum of the blue and gray areas combined represents all S-sites available on **CoP** that we can probe by the three SPR_3 reagents. We use rectangular areas in this graphic representation for simplicity. Please note, however, that the distribution of sites *within* a certain BDFE range is not known, and the number of sites is not necessarily equally distributed within that BDFE range as would be suggested by rectangular areas. The shaded area corresponds to the amount of sulfur that cannot be removed by P^nBu_3. The question mark indicates that there may be S-sites available on **CoP** with BDFEs < 69 kcal/mol, but this cannot be probed with this specific series of three SPR_3 reagents used herein.

that SP^nBu_3 could not add S to **CoP** suggests an upper limit of 84 kcal/mol for the bond strengths to S that can be formed on **CoP**. The amount of S added to **CoP** by $SPPh_3$ of 0.09 equiv per surface "CoP" suggests that this many S-sites are available on **CoP** that can bind S with bond strengths higher than 76 kcal/mol but lower than 84 kcal/mol. TriMePS added ∼1.5 times as much S to **CoP** as $SPPh_3$, suggesting that 0.14 site per surface "CoP" unit can bind S with bond strengths between 69 and 84 kcal/mol. About 65% of these sites can be filled from S-transfer with $SPPh_3$ with bond strengths between 76 and 84 kcal/mol, and ∼35% of these sites have lower bond strengths between 69 and 76 kcal/mol. In Figure 6 we schematically represent the S-sites available for each BDFE range limited by the different PR_3/SPR_3 couples. Please note that while the reaction with SP^nBu_3 provided an upper limit of the S-binding strengths on **CoP** that is possible under these conditions, our series of three SPR_3 reagents does not necessarily probe the weakest S bond on **CoP** possible: S-sites on **CoP** with BDFEs < 69 kcal/mol may exist but could only be probed with S-transfer reagents having weaker P═S bonds. However, the strategy we report here can likely be employed for other SPR_3 reagents with alternative P═S strengths and could thereby

https://doi.org/10.1021/jacs.3c07312
J. Am. Chem. Soc. 2023, 145, 23556−23567

provide more detailed information about the BDFE distribution.

Our equilibration results of the reaction of S-modified **CoP**-$\mathbf{S}_x$ with P^nBu_3 showed that the S-modification is, in part, reversible: Some of the S on **CoP** can be removed by reaction with P^nBu_3 but not all. This is consistent with a prior report suggesting the presence of both reversibly and irreversibly bound sulfur on transition metal phosphides.[21] Since we used a large excess of P^nBu_3 and let the reaction equilibrate, the partial sulfur removal is likely a thermodynamic rather than a kinetic effect (similar to our S-addition equilibration reactions that also probe thermodynamic properties). Our observation that no S could be added with SP^nBu_3 seems to exclude the possibility that **CoP** binds S more strongly than P^nBu_3. However, XPS analysis of **CoP**-$\mathbf{S}_{x\text{-}y}$ obtained after reaction of **CoP**-$\mathbf{S}_x$ with P^nBu_3 showed partial oxidation of the **CoP** surface, which could influence the S-binding on **CoP**. It is hence possible that some of the S added to **CoP** with a BDFE smaller than 84 kcal/mol (shaded area in Figure 6) are converted into S-sites with BDFEs larger than 84 kcal/mol by surface oxidation. Another possibility would be that the sulfur that cannot be removed by P^nBu_3 corresponds to S-sites that are sterically not accessible to P^nBu_3, perhaps because of the surface oxidation or diffusion of S to the interior of the **CoP** particles. However, while anion diffusion or P/S anion mixing in materials is generally conceivable via a Kirkendall mechanism, it is more typically observed in nanomaterials and usually requires higher temperatures of ~200−350 °C rather than the 80 °C used herein.[68−70] In view of the XPS data of the **CoP**-$\mathbf{S}_{x\text{-}y}$ after S-removal providing clear evidence for residual S-content at the surface and the surface being oxidized, surface oxidation is the more likely explanation. Hence, while we cannot absolutely exclude the possibility that a very small amount of sulfur could diffuse to the inside of the **CoP** particles, the observed partial sulfur removal is probably due to surface oxidation.

In summary, *our CoP-modification approach with molecular SPR_3 reagents has provided a first experimental estimate of the distribution of thermochemical properties of sulfur binding to* ***CoP***. While there is some uncertainty in the absolute BDFE values that can be derived by this method, the general thermochemical distribution of BDFEs on **CoP** is more accurate. These thermochemical data could be of key relevance for (electro-)catalysis. For example, metal−sulfur bond energies have been shown to correlate with catalytic activity in hydrodesulfurization via the so-called volcano plots (although, the validity of such plots is debated[71,72]).[73−76] The sulfur bond energies in these volcano plots are typically derived from bulk properties of sulfides or from DFT calculations on crystalline facet models of surfaces with limited relevance to the complex amorphous surfaces of real catalysts. Our method and data for **CoP** hence provide an *experimental measure of sulfur binding on an amorphous transition metal phosphide surface that could be directly predictive for their hydrodesulfurization activity*. This is subject of further investigation.

Structure of S-Sites on CoP. The thermochemical data discussed above indicate that there are different types of S-sites on the amorphous **CoP** surface. This site distribution could include S on top of Co or P surface atoms, S bridging multiple Co and/or P atoms, and/or S-sites that differ in their environment beyond the first coordination sphere. XPS data of **CoP**-$\mathbf{S}_x$ do not allow clear structural insight, as the observed S 2p signals at roughly 160−163 eV are consistent with S-binding that involves Co but also with terminal P═S sites in view of reported XPS data of cobalt sulfides and phosphosulfides[77−80] and of XPS data of molecular SPR_3 reagents (SI). S binding to Co-based sites would be in line with reported studies on S-transfer to Co_xP_y clusters in the gas phase[81] and the M−S bond formation reported for metal phosphide hydrodesulfurization catalysts.[5] However, P on **CoP** surfaces could also contribute to S-binding considering the reported capability of P on metal phosphides to bind CO and aryl groups.[22,82] DFT calculations on single crystalline facets of cobalt phosphide and other transition metal phosphides suggest that S bridging multiple Co atoms and perhaps also involving a P atom could be the energetically most favorable S-sites.[12−14,19,83−85] However, single crystalline facet models of phosphide surfaces can likely not capture the diversity of S-sites exhibited by the amorphous **CoP** studied herein.[86] The **CoP** surface is likely complex with defects, nonstoichiometries, residual PO_x and P−OH, and surface hydrogen.[54] More realistic computational models are needed for detailed atomic-level insight into the ensemble of S-sites present on **CoP**. We propose that the thermochemical data obtained herein that describe the site distribution on an amorphous **CoP** surface could provide valuable experimental benchmark values for the development of such new computational models.

S-Effect on the Catalytic Hydrogenation by CoP. The controlled introduction of sulfur to transition metal phosphides developed herein can also be a tool to *understand the S-effect in transition metal phosphides for HER and hydrotreating* (electro-)catalysis by experimentally accessing the role of different S-sites on **CoP** in catalysis separately. For a better understanding of the effect of sulfur on the hydrogenation catalysis by phosphides, we have tested S-modified **CoP** (**CoP**-$\mathbf{S}_{0.09}$ and **CoP**-$\mathbf{S}_{0.14}$) and the bare **CoP** in the catalysis of cinnamaldehyde hydrogenation. Our results show that the production of HCAL and COL was enhanced when **CoP** has some exposed sulfur on the surface (Scheme 1), but the initial activity was likely decreased especially with too much sulfur. This is reminiscent of prior reports of S-effects in the electrocatalytic HER by transition metal phosphides, suggesting an intermediate amount of S-doping is optimal for catalytic activity.[12,15] This might also explain what seems to be inconsistent literature on the S-effect in the hydrotreating

Scheme 1. Possible Reaction Pathways for Cinnamaldehyde (CAL) under Hydrogenation Conditions[a]

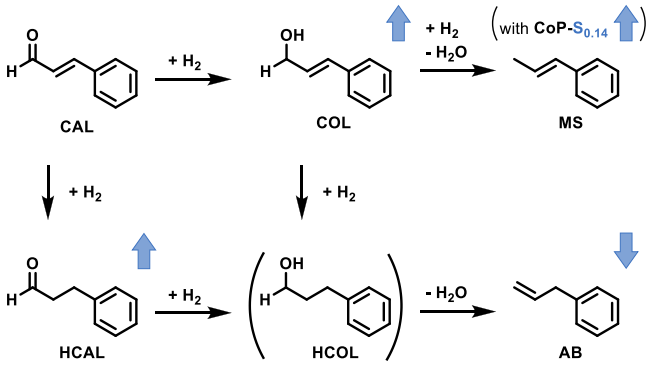

[a]The effect of sulfur on **CoP** for **CoP**-$\mathbf{S}_{0.09}$ and **CoP**-$\mathbf{S}_{0.14}$ on catalytic productivity is shown as blue arrows next to the products COL, HCAL, and AB. MS productivity was only changed with large amounts of S on **CoP**, i.e., with **CoP**-$\mathbf{S}_{0.14}$ but not with **CoP**-$\mathbf{S}_{0.09}$.

https://doi.org/10.1021/jacs.3c07312
J. Am. Chem. Soc. 2023, 145, 23556−23567

catalysis by transition metal phosphides: while most studies report a promoting effect of S on activity,[22−28] some suggest that H_2S in the feed or large sulfur contents at the surface (>0.17 S per surface metal) can decrease their catalytic activity.[31−33]

In addition to the effect on productivity, sulfur on **CoP** also influenced the selectivity in the catalytic hydrogenation of cinnamaldehyde hydrogenation. In line with the known ability of transition metal phosphides to catalyze the hydrogenation of multiple bonds and the hydrodeoxygenation of bio-oils,[18,63−66,87−93] hydrogenation products (HCAL and COL) as well as hydrodeoxygenation products (AB and MS) were formed with all catalysts. Both **CoP-S$_x$** and especially **CoP-S$_{0.14}$** showed higher productivity for HCAL than that of the bare **CoP**. With the bare **CoP**, COL was a primary product as well as an intermediate, and the initially formed amount of COL decreased again after going through a maximum. With both **CoP-S$_x$**, on the other hand, the initially formed amount of COL stayed relatively constant, suggesting that a follow-up reaction of COL was hindered in the presence of surface sulfur. We observed a decreased formation of AB with **CoP-S$_x$** compared to the bare **CoP**. The MS production was a bit higher with **CoP-S$_{0.14}$**. Prior literature on cinnamaldehyde hydrogenation suggests that AB is formed via dehydration of hydrocinnamyl alcohol (HCOL, not observed herein), and MS may be formed via hydrogenolysis of COL (Scheme 1).[94−97] This would suggest that sulfur on **CoP-S$_x$** disfavors the dehydration pathway (or perhaps the full hydrogenation to HCOL), but not the hydrogenolysis of COL to MS.

The observed effect of surface sulfur on the reaction selectivity could be explained by the interaction of sulfur with acidic sites on **CoP**. It has previously been reported that transition metal phosphides can expose both metallic and acidic sites.[64,87−89,91,93,98,99] The acidic sites on phosphides (either Lewis acidic sites of $M^{\delta+}$ or P-OH Brønsted acidic sites at the surface) are thought to catalyze dehydration reactions, while metallic sites (M or $M^{\delta+}$ sites that exhibit metallic properties through electron delocalization) are mainly responsible for hydrogenation reactions.[87−90,92,98−100] We speculate that sulfur poisoned such $Co^{\delta+}$ and/or P-OH acidic sites on **CoP** that are responsible for the dehydration of HCOL to AB but enhanced the catalytic productivity of the metallic sites responsible for catalytic hydrogenation. We attempted to quantify the number of acidic sites by IR probes, but this was unsuccessful due to the low IR reflectivity of cobalt phosphide, as previously reported for other unsupported transition metal phosphides.[88] In addition, prior studies suggest that chemisorption experiments cannot be used to put catalytic productivity into context with active site densities in the case of transition metal phosphides of different composition.[22,32,101−103] However, the proposed enhanced hydrogenation productivity of metallic sites is similar to prior reports suggesting enhanced stability or optimized H-binding energies with S-doped phosphides,[9,10,12−17,30] but this is subject of further investigation.

Our data hence show a clear S-effect on the catalytic productivity and selectivity of cobalt phosphide in cinnamaldehyde hydrogenation. We propose that the ensemble of different sulfur sites on **CoP** acts in a dual role leading to both desired and undesired effects: (1) S could poison acidic sites responsible for AB formation (desired effect on selectivity) but also some of the metallic sites for hydrogenation, leading to a decreased initial activity (undesired effect on activity). (2) S near an unblocked active site could also enhance catalytic productivity of hydrogenation (desired effect on activity or stability) and of hydrogenolysis (undesired effect on selectivity). The details of the mechanism are currently unknown. However, similar dual roles of sulfur as both poison and promoter have previously been reported for other heterogeneous catalysts, including metal catalysts for hydrogenations.[29,104] The effects observed herein depended on the number and type of S on **CoP**. **CoP-S$_{0.09}$** provided the best balance of desired and undesired effects, because it showed enhanced productivity and selectivity for hydrogenation products without the significantly decreased initial activity and the increased secondary product formation (MS) shown by **CoP-S$_{0.14}$**. Combined, *the best overall catalytic performance for hydrogenation was hence obtained with an intermediate amount of sulfur having intermediate binding strengths on the **CoP** surface—some but not too much sulfur*.

CONCLUSION

We present a new method for modifying **CoP** with sulfur using molecular S-transfer reagents. Our method enabled the controlled addition of a varied amount of sulfur to the surface of **CoP** that is in part reversible. We further showed that there is a distribution of sulfur sites possible on the surface of **CoP** with binding energies ranging from 69 to 84 kcal/mol. Roughly 65% of the sulfur bound within this energy range had binding energies between 76 and 84 kcal/mol, while the other 35% was bound with strengths of 69 to 76 kcal/mol. The molecular-like equilibrations used here allowed for an experimental assessment of the distribution of binding energies on a complex, amorphous **CoP** surface, which is highly complementary to the information amenable through more standard DFT calculations on facet models. Metal−sulfur bond energies have previously been shown to correlate with the hydrodesulfurization activity of some catalysts in the so-called volcano plots. The thermochemical data obtained here could be used to probe the predictive power of analogous bond energy−hydrodesulfurization activity plots for transition metal phosphides.

In light of the reported effect of sulfur in S-doped transition metal phosphides on hydrotreating and water splitting catalysis, we probed the effect of the sulfur content in the catalytic hydrogenation of cinnamaldehyde by **CoP**. We showed that the best balance of catalytic properties for hydrogenation is obtained with some but not too much sulfur at the **CoP** surface and with sulfur that has intermediate binding strengths on the surface. The enhancement of the catalytic properties of **CoP** through the controlled addition of sulfur to the phosphide surface opens exciting avenues for the development of transition metal phosphides in catalytic applications.

ASSOCIATED CONTENT

Supporting Information

The Supporting Information is available free of charge at https://pubs.acs.org/doi/10.1021/jacs.3c07312.

Detailed experimental procedures, SEM images, EDX and elemental analysis data, BET measurements, XPS, pXRD, and NMR spectra, discussion of P═S bond strengths, discussion of NMR analysis, catalysis (PDF)

https://doi.org/10.1021/jacs.3c07312
J. Am. Chem. Soc. 2023, 145, 23556−23567

AUTHOR INFORMATION

Corresponding Author

Murielle F. Delley − *Department of Chemistry, University of Basel, 4058 Basel, Switzerland;* orcid.org/0000-0001-6450-5540; Email: murielle.delley@unibas.ch

Authors

Nina A. Arnosti − *Department of Chemistry, University of Basel, 4058 Basel, Switzerland*

Vanessa Wyss − *Department of Chemistry, University of Basel, 4058 Basel, Switzerland;* orcid.org/0000-0003-2514-189X

Complete contact information is available at: https://pubs.acs.org/10.1021/jacs.3c07312

Notes

The authors declare no competing financial interest.

ACKNOWLEDGMENTS

We thank Prof. Daniel Häussinger for measuring T1 relaxation times and for help with NMR measurements. We thank Dr. Laurent Marot for help with XPS measurements, Dr. Alessandro Prescimone for assistance with powder X-ray diffraction, and Eva Bieler and Susanne Erpel of the Nano Imaging Lab, Swiss Nanoscience Institute (SNI), University of Basel, for support with scanning electron microscopy and energy-dispersive X-ray diffraction measurements. We gratefully acknowledge financial support from the Swiss National Science Foundation (SNSF) via an SNSF PRIMA fellowship granted to M.F.D. (PR00P2_193103) and from The Branco Weiss Fellowship − Society in Science, administered by the ETH Zürich granted to M.F.D.

REFERENCES

(1) Oyama, S. T.; Gott, T.; Zhao, H.; Lee, Y.-K. Transition metal phosphide hydroprocessing catalysts: A review. *Catal. Today* **2009**, *143* (1), 94−107.

(2) Morales-Guio, C. G.; Stern, L.-A.; Hu, X. Nanostructured hydrotreating catalysts for electrochemical hydrogen evolution. *Chem. Soc. Rev.* **2014**, *43* (18), 6555−6569.

(3) Shi, Y.; Zhang, B. Recent advances in transition metal phosphide nanomaterials: synthesis and applications in hydrogen evolution reaction. *Chem. Soc. Rev.* **2016**, *45* (6), 1529−1541.

(4) Zhao, H.; Yuan, Z.-Y. Transition metal-phosphorus-based materials for electrocatalytic energy conversion reactions. *Catal. Sci. Technol.* **2017**, *7* (2), 330−347.

(5) Oyama, S. T. Novel catalysts for advanced hydroprocessing: transition metal phosphides. *J. Catal.* **2003**, *216* (1), 343−352.

(6) Callejas, J. F.; Read, C. G.; Roske, C. W.; Lewis, N. S.; Schaak, R. E. Synthesis, Characterization, and Properties of Metal Phosphide Catalysts for the Hydrogen-Evolution Reaction. *Chem. Mater.* **2016**, *28* (17), 6017−6044.

(7) El-Refaei, S. M.; Russo, P. A.; Pinna, N. Recent Advances in Multimetal and Doped Transition-Metal Phosphides for the Hydrogen Evolution Reaction at Different pH values. *ACS Appl. Mater. Interfaces* **2021**, *13* (19), 22077−22097.

(8) Sun, Y.; Zhang, T.; Li, C.; Xu, K.; Li, Y. Compositional engineering of sulfides, phosphides, carbides, nitrides, oxides, and hydroxides for water splitting. *J. Mater. Chem. A* **2020**, *8* (27), 13415−13436.

(9) Kibsgaard, J.; Jaramillo, T. F. Molybdenum Phosphosulfide: An Active, Acid-Stable, Earth-Abundant Catalyst for the Hydrogen Evolution Reaction. *Angew. Chem., Int. Ed.* **2014**, *53* (52), 14433−14437.

(10) Cabán-Acevedo, M.; Stone, M. L.; Schmidt, J. R.; Thomas, J. G.; Ding, Q.; Chang, H.-C.; Tsai, M.-L.; He, J.-H.; Jin, S. Efficient hydrogen evolution catalysis using ternary pyrite-type cobalt phosphosulphide. *Nat. Mater.* **2015**, *14* (12), 1245−1251.

(11) Liu, W.; Hu, E.; Jiang, H.; Xiang, Y.; Weng, Z.; Li, M.; Fan, Q.; Yu, X.; Altman, E. I.; Wang, H. A highly active and stable hydrogen evolution catalyst based on pyrite-structured cobalt phosphosulfide. *Nat. Commun.* **2016**, *7* (1), 10771.

(12) Liang, K.; Pakhira, S.; Yang, Z.; Nijamudheen, A.; Ju, L.; Wang, M.; Aguirre-Velez, C. I.; Sterbinsky, G. E.; Du, Y.; Feng, Z.; Mendoza-Cortes, J. L.; Yang, Y. S-Doped MoP Nanoporous Layer Toward High-Efficiency Hydrogen Evolution in pH-Universal Electrolyte. *ACS Catal.* **2019**, *9* (1), 651−659.

(13) Anjum, M. A. R.; Bhatt, M. D.; Lee, M. H.; Lee, J. S. Sulfur-Doped Dicobalt Phosphide Outperforming Precious Metals as a Bifunctional Electrocatalyst for Alkaline Water Electrolysis. *Chem. Mater.* **2018**, *30* (24), 8861−8870.

(14) Anjum, M. A. R.; Okyay, M. S.; Kim, M.; Lee, M. H.; Park, N.; Lee, J. S. Bifunctional sulfur-doped cobalt phosphide electrocatalyst outperforms all-noble-metal electrocatalysts in alkaline electrolyzer for overall water splitting. *Nano Energy* **2018**, *53*, 286−295.

(15) Chang, J.; Li, K.; Wu, Z.; Ge, J.; Liu, C.; Xing, W. Sulfur-Doped Nickel Phosphide Nanoplates Arrays: A Monolithic Electrocatalyst for Efficient Hydrogen Evolution Reactions. *ACS Appl. Mater. Interfaces* **2018**, *10* (31), 26303−26311.

(16) Ye, R.; del Angel-Vicente, P.; Liu, Y.; Arellano-Jimenez, M. J.; Peng, Z.; Wang, T.; Li, Y.; Yakobson, B. I.; Wei, S.-H.; Yacaman, M. J.; Tour, J. M. High-Performance Hydrogen Evolution from $MoS_{2(1-x)}P_x$ Solid Solution. *Adv. Mater.* **2016**, *28* (7), 1427−1432.

(17) Huang, Y.; Song, X.; Deng, J.; Zha, C.; Huang, W.; Wu, Y.; Li, Y. Ultra-dispersed molybdenum phosphide and phosphosulfide nanoparticles on hierarchical carbonaceous scaffolds for hydrogen evolution electrocatalysis. *Appl. Catal. B: Environ.* **2019**, *245*, 656−661.

(18) Oyama, S. T.; Wang, X.; Lee, Y. K.; Chun, W. J. Active phase of Ni_2P/SiO_2 in hydroprocessing reactions. *J. Catal.* **2004**, *221* (2), 263−273.

(19) Vidal, A. B.; Peña-Mena, J. L.; Hurtado-Aular, O.; Añez, R.; Sierraalta, A. Unraveling the Structure and Surface Chemistry of the Phosphosulfide Phase Formed on Ni_2P under Hydrodesulfurization Reaction Conditions: A DFT Study. *J. Phys. Chem. C* **2022**, *126* (33), 14187−14200.

(20) Bando, K. K.; Wada, T.; Miyamoto, T.; Miyazaki, K.; Takakusagi, S.; Koike, Y.; Inada, Y.; Nomura, M.; Yamaguchi, A.; Gott, T.; Oyama, S. T.; Asakura, K. Combined in situ QXAFS and FTIR analysis of a Ni phosphide catalyst under hydrodesulfurization conditions. *J. Catal.* **2012**, *286*, 165−171.

(21) Wu, Z.; Sun, F.; Wu, W.; Feng, Z.; Liang, C.; Wei, Z.; Li, C. On the surface sites of MoP/SiO_2 catalyst under sulfiding conditions: IR spectroscopy and catalytic reactivity studies. *J. Catal.* **2004**, *222* (1), 41−52.

(22) Layman, K. A.; Bussell, M. E. Infrared Spectroscopic Investigation of CO Adsorption on Silica-Supported Nickel Phosphide Catalysts. *J. Phys. Chem. B* **2004**, *108* (30), 10930−10941.

(23) Oyama, S. T.; Wang, X.; Lee, Y. K.; Bando, K.; Requejo, F. G. Effect of Phosphorus Content in Nickel Phosphide Catalysts Studied by XAFS and Other Techniques. *J. Catal.* **2002**, *210* (1), 207−217.

(24) Duan, X.; Teng, Y.; Wang, A.; Kogan, V. M.; Li, X.; Wang, Y. Role of sulfur in hydrotreating catalysis over nickel phosphide. *J. Catal.* **2009**, *261* (2), 232−240.

(25) Cecilia, J. A.; Infantes-Molina, A.; Rodríguez-Castellón, E.; Jiménez-López, A. A novel method for preparing an active nickel phosphide catalyst for HDS of dibenzothiophene. *J. Catal.* **2009**, *263* (1), 4−15.

(26) Tian, S.; Li, X.; Wang, A.; Chen, Y.; Li, H.; Hu, Y. Hydrodenitrogenation of Quinoline and Decahydroquinoline Over a Surface Nickel Phosphosulfide Phase. *Catal. Lett.* **2018**, *148* (6), 1579−1588.

(27) Prins, R.; Bussell, M. E. Metal Phosphides: Preparation, Characterization and Catalytic Reactivity. *Catal. Lett.* **2012**, *142* (12), 1413−1436.
(28) Tian, S.; Li, X.; Wang, A.; Prins, R.; Chen, Y.; Hu, Y. Facile Preparation of Ni_2P with a Sulfur-Containing Surface Layer by Low-Temperature Reduction of $Ni_2P_2S_6$. *Angew. Chem., Int. Ed.* **2016**, *55* (12), 4030−4034.
(29) McCue, A. J.; Anderson, J. A. Sulfur as a catalyst promoter or selectivity modifier in heterogeneous catalysis. *Catal. Sci. Technol.* **2014**, *4* (2), 272−294.
(30) Ghadge, S. D.; Velikokhatnyi, O. I.; Datta, M. K.; Shanthi, P. M.; Kumta, P. N. Computational and experimental investigation of Co and S-doped Ni_2P as an efficient electrocatalyst for acid mediated proton exchange membrane hydrogen evolution reaction. *Catal. Sci. Technol.* **2021**, *11* (3), 861−873.
(31) Bowker, R. H.; Layan Savithra, G. H.; Carrillo, B. A.; Hubach, K. G.; McDonald, T.; Brock, S. L.; Bussell, M. E. Effect of particle size on the sulfur resistance of nickel phosphide hydrodesulfurization catalysts. *J. Catal.* **2023**, *425*, 70−79.
(32) Yang, S.; Liang, C.; Prins, R. A novel approach to synthesizing highly active Ni_2P/SiO_2 hydrotreating catalysts. *J. Catal.* **2006**, *237* (1), 118−130.
(33) Stinner, C.; Prins, R.; Weber, T. Binary and Ternary Transition-Metal Phosphides as HDN Catalysts. *J. Catal.* **2001**, *202* (1), 187−194.
(34) Anjum, M. A. R.; Lee, J. S. Sulfur and Nitrogen Dual-Doped Molybdenum Phosphide Nanocrystallites as an Active and Stable Hydrogen Evolution Reaction Electrocatalyst in Acidic and Alkaline Media. *ACS Catal.* **2017**, *7* (4), 3030−3038.
(35) Wu, Z.; Li, X.; Liu, W.; Zhong, Y.; Gan, Q.; Li, X.; Wang, H. Materials Chemistry of Iron Phosphosulfide Nanoparticles: Synthesis, Solid State Chemistry, Surface Structure, and Electrocatalysis for the Hydrogen Evolution Reaction. *ACS Catal.* **2017**, *7* (6), 4026−4032.
(36) Qi, Y.; Zhang, L.; Sun, L.; Chen, G.; Luo, Q.; Xin, H.; Peng, J.; Li, Y.; Ma, F. Sulfur doping enhanced desorption of intermediates on NiCoP for efficient alkaline hydrogen evolution. *Nanoscale* **2020**, *12* (3), 1985−1993.
(37) Saadi, F. H.; Carim, A. I.; Drisdell, W. S.; Gul, S.; Baricuatro, J. H.; Yano, J.; Soriaga, M. P.; Lewis, N. S. Operando Spectroscopic Analysis of CoP Films Electrocatalyzing the Hydrogen-Evolution Reaction. *J. Am. Chem. Soc.* **2017**, *139* (37), 12927−12930.
(38) Strunk, J.; Bañares, M. A.; Wachs, I. E. Vibrational Spectroscopy of Oxide Overlayers. *Top. Catal.* **2017**, *60* (19), 1577−1617.
(39) Bergmann, A.; Martinez-Moreno, E.; Teschner, D.; Chernev, P.; Gliech, M.; de Araújo, J. F.; Reier, T.; Dau, H.; Strasser, P. Reversible amorphization and the catalytically active state of crystalline Co_3O_4 during oxygen evolution. *Nat. Commun.* **2015**, *6* (1), 8625.
(40) Merki, D.; Fierro, S.; Vrubel, H.; Hu, X. Amorphous molybdenum sulfide films as catalysts for electrochemical hydrogen production in water. *Chem. Sci.* **2011**, *2* (7), 1262−1267.
(41) Murray, C.; Norris, D. J.; Bawendi, M. G. Synthesis and characterization of nearly monodisperse CdE (E= sulfur, selenium, tellurium) semiconductor nanocrystallites. *J. Am. Chem. Soc.* **1993**, *115* (19), 8706−8715.
(42) Liu, H.; Owen, J. S.; Alivisatos, A. P. Mechanistic Study of Precursor Evolution in Colloidal Group II-VI Semiconductor Nanocrystal Synthesis. *J. Am. Chem. Soc.* **2007**, *129* (2), 305−312.
(43) Ruberu, T. P. A.; Albright, H. R.; Callis, B.; Ward, B.; Cisneros, J.; Fan, H.-J.; Vela, J. Molecular Control of the Nanoscale: Effect of Phosphine-Chalcogenide Reactivity on CdS-CdSe Nanocrystal Composition and Morphology. *ACS Nano* **2012**, *6* (6), 5348−5359.
(44) García-Rodríguez, R.; Hendricks, M. P.; Cossairt, B. M.; Liu, H.; Owen, J. S. Conversion Reactions of Cadmium Chalcogenide Nanocrystal Precursors. *Chem. Mater.* **2013**, *25* (8), 1233−1249.
(45) Sowers, K. L.; Swartz, B.; Krauss, T. D. Chemical Mechanisms of Semiconductor Nanocrystal Synthesis. *Chem. Mater.* **2013**, *25* (8), 1351−1362.
(46) Thompson, K. L.; Katzbaer, R. R.; Terrones, M.; Schaak, R. E. Formation and Transformation of $Cu_{2-x}Se_{1-y}Te_y$ Nanoparticles Synthesized by Tellurium Anion Exchange of Copper Selenide. *Inorg. Chem.* **2023**, *62* (11), 4550−4557.
(47) Garcia-Herrera, L. F.; McAllister, H. P.; Xiong, H.; Wang, H.; Lord, R. W.; O'Boyle, S. K.; Imamovic, A.; Steimle, B. C.; Schaak, R. E.; Plass, K. E. Multistep Regioselectivity and Non-Kirkendall Anion Exchange of Copper Chalcogenide Nanorods. *Chem. Mater.* **2021**, *33* (10), 3841−3850.
(48) Hall, K. A.; Mayer, J. M. Reactions of ML_4Cl_2 (M= Mo, W; L= PMe_3, $PMePh_2$) with epoxides, episulfides, carbon dioxide, hetero-cumulenes, and other substrates: a comparative study of oxidative addition by oxygen atom, sulfur atom, or nitrene group transfer. *J. Am. Chem. Soc.* **1992**, *114* (26), 10402−10411.
(49) McDonough, J. E.; Mendiratta, A.; Curley, J. J.; Fortman, G. C.; Fantasia, S.; Cummins, C. C.; Rybak-Akimova, E. V.; Nolan, S. P.; Hoff, C. D. Thermodynamic, Kinetic, and Computational Study of Heavier Chalcogen (S, Se, and Te) Terminal Multiple Bonds to Molybdenum, Carbon, and Phosphorus. *Inorg. Chem.* **2008**, *47* (6), 2133−2141.
(50) Lohrey, T. D.; Cortes, E. A.; Fostvedt, J. I.; Oanta, A. K.; Jain, A.; Bergman, R. G.; Arnold, J. Diverse Reactivity of a Rhenium(V) Oxo Imido Complex: [2 + 2] Cycloadditions, Chalcogen Metathesis, Oxygen Atom Transfer, and Protic and Hydridic 1,2-Additions. *Inorg. Chem.* **2020**, *59* (15), 11096−11107.
(51) Ward, J. P.; Lim, P. J.; Evans, D. J.; White, J. M.; Young, C. G. Tungsten Ligand-Based Sulfur-Atom-Transfer Catalysts: Synthesis, Characterization, Sustained Anaerobic Catalysis, and Mode of Aerial Deactivation. *Inorg. Chem.* **2020**, *59* (23), 16824−16828.
(52) Ott, J. C.; Wadepohl, H.; Gade, L. H. Metalloradical Reactivity, Charge Transfer, and Atom Abstractions in a T-Shaped Iron(I) Complex. *Inorg. Chem.* **2021**, *60* (6), 3927−3938.
(53) Wu, Z.; Gan, Q.; Li, X.; Zhong, Y.; Wang, H. Elucidating Surface Restructuring-Induced Catalytic Reactivity of Cobalt Phosphide Nanoparticles under Electrochemical Conditions. *J. Phys. Chem. C* **2018**, *122* (5), 2848−2853.
(54) Delley, M. F.; Wu, Z.; Mundy, M. E.; Ung, D.; Cossairt, B. M.; Wang, H.; Mayer, J. M. Hydrogen on Cobalt Phosphide. *J. Am. Chem. Soc.* **2019**, *141* (38), 15390−15402.
(55) Capps, K. B.; Wixmerten, B.; Bauer, A.; Hoff, C. D. Thermochemistry of Sulfur Atom Transfer. Enthalpies of Reaction of Phosphines with Sulfur, Selenium, and Tellurium, and of Desulfurization of Triphenylarsenic Sulfide, Triphenylantimony Sulfide, and Benzyl Trisulfide. *Inorg. Chem.* **1998**, *37* (12), 2861−2864.
(56) Alvarado, S. R.; Shortt, I. A.; Fan, H.-J.; Vela, J. Assessing Phosphine-Chalcogen Bond Energetics from Calculations. *Organometallics* **2015**, *34* (16), 4023−4031.
(57) Chernick, C. L.; Pedley, J. B.; Skinner, H. A. 350. Thermochemistry of organophosphorus compounds. Part III. The heat of addition of sulphur to triethyl phosphite, and to tri-n-propyl- and tri-n-butyl-phosphine. *J. Chem. Soc.* **1957**, 1851−1854.
(58) Mortimer, C. T. The thermochemistry of organo-phosphorus compounds. *Pure Appl. Chem.* **1961**, *2* (1−2), 71−76.
(59) Schneider, W.; Thiel, W.; Komornicki, A. Ab initio calculation of harmonic force fields and vibrational spectra for the phosphine oxides and sulfides R_3PY (R = H, F, CH_3; Y = O, S). *J. Phys. Chem.* **1988**, *92* (20), 5611−5619.
(60) Ibdah, A.; Espenson, J. H.; Jenks, W. S. Computational Study of Sulfur Atom-Transfer Reactions from Thiiranes to ER_3 (E = As, P; R = CH_3, Ph). *Inorg. Chem.* **2005**, *44* (23), 8426−8432.
(61) NIST webbook for S°(S). https://webbook.nist.gov/cgi/cbook.cgi?ID=C7704349&Units=SI&Mask=1EFF (accessed 2023−05−12).
(62) Gan, Q.; Wu, Z.; Li, X.; Liu, W.; Wang, H. Structure and Electrocatalytic Reactivity of Cobalt Phosphosulfide Nanomaterials. *Top. Catal.* **2018**, *61* (9), 958−964.
(63) Wang, H.; Shu, Y.; Zheng, M.; Zhang, T. Selective Hydrogenation of Cinnamaldehyde to Hydrocinnamaldehyde over

SiO_2 Supported Nickel Phosphide Catalysts. *Catal. Lett.* **2008**, *124* (3), 219−225.
(64) Bonita, Y.; Jain, V.; Geng, F.; O'Connell, T. P.; Ramos, N. X.; Rai, N.; Hicks, J. C. Hydrogenation of cinnamaldehyde to cinnamyl alcohol with metal phosphides: Catalytic consequences of product and pyridine doping. *Appl. Catal. B: Environ.* **2020**, *277*, 119272.
(65) Liu, P.; Zhu, Y.-L.; Zhou, L.; Zhang, W.-H.; Li, Y.-X. Amorphous Nickel Phosphide Nanoparticles for Selective Hydrogenation of Cinnamaldehyde. *Catal. Lett.* **2020**, *150* (9), 2695−2702.
(66) Ishikawa, H.; Sheng, M.; Nakata, A.; Nakajima, K.; Yamazoe, S.; Yamasaki, J.; Yamaguchi, S.; Mizugaki, T.; Mitsudome, T. Air-Stable and Reusable Cobalt Phosphide Nanoalloy Catalyst for Selective Hydrogenation of Furfural Derivatives. *ACS Catal.* **2021**, *11* (2), 750−757.
(67) Kuo, D.-Y.; Nishiwaki, E.; Rivera-Maldonado, R. A.; Cossairt, B. M. The Role of Hydrogen Adsorption Site Diversity in Catalysis on Transition-Metal Phosphide Surfaces. *ACS Catal.* **2023**, *13* (1), 287−295.
(68) Hong, Y.; Kim, T.; Jo, J.; Kim, B.; Jin, H.; Baik, H.; Lee, K. Highly Crystalline Hollow Toroidal Copper Phosphosulfide via Anion Exchange: A Versatile Cation Exchange Nanoplatform. *ACS Nano* **2020**, *14* (9), 11205−11214.
(69) Ha, D.-H.; Moreau, L. M.; Bealing, C. R.; Zhang, H.; Hennig, R. G.; Robinson, R. D. The structural evolution and diffusion during the chemical transformation from cobalt to cobalt phosphide nanoparticles. *J. Mater. Chem.* **2011**, *21* (31), 11498−11510.
(70) Xu, Y.; Wu, R.; Zhang, J.; Shi, Y.; Zhang, B. Anion-exchange synthesis of nanoporous FeP nanosheets as electrocatalysts for hydrogen evolution reaction. *Chem. Commun.* **2013**, *49* (59), 6656−6658.
(71) Quaino, P.; Juarez, F.; Santos, E.; Schmickler, W. Volcano plots in hydrogen electrocatalysis - uses and abuses. *Beilstein J. Nanotechnol.* **2014**, *5*, 846−854.
(72) Zeradjanin, A. R.; Grote, J.-P.; Polymeros, G.; Mayrhofer, K. J. J. A Critical Review on Hydrogen Evolution Electrocatalysis: Re-exploring the Volcano-relationship. *Electroanalysis* **2016**, *28* (10), 2256−2269.
(73) Seh, Z. W.; Kibsgaard, J.; Dickens, C. F.; Chorkendorff, I.; Nørskov, J. K.; Jaramillo, T. F. Combining theory and experiment in electrocatalysis: Insights into materials design. *Science* **2017**, *355* (6321), No. eaad4998.
(74) Nørskov, J. K.; Abild-Pedersen, F.; Studt, F.; Bligaard, T. Density functional theory in surface chemistry and catalysis. *Proc. Natl. Acad. Sci. U.S.A.* **2011**, *108* (3), 937−943.
(75) Toulhoat, H.; Raybaud, P. Kinetic interpretation of catalytic activity patterns based on theoretical chemical descriptors. *J. Catal.* **2003**, *216* (1), 63−72.
(76) Toulhoat, H.; Raybaud, P.; Kasztelan, S.; Kresse, G.; Hafner, J. Transition metals to sulfur binding energies relationship to catalytic activities in HDS: back to Sabatier with first principle calculations. *Catal. Today* **1999**, *50* (3), 629−636.
(77) Fan, K.; Zou, H.; Lu, Y.; Chen, H.; Li, F.; Liu, J.; Sun, L.; Tong, L.; Toney, M. F.; Sui, M.; Yu, J. Direct Observation of Structural Evolution of Metal Chalcogenide in Electrocatalytic Water Oxidation. *ACS Nano* **2018**, *12* (12), 12369−12379.
(78) Korányi, T. I. Phosphorus promotion of Ni (Co)-containing Mo-free catalysts in thiophene hydrodesulfurization. *Appl. Catal. A: Gen.* **2003**, *239* (1), 253−267.
(79) Chanturiya, V. A.; Bunin, I. Z.; Ryazantseva, M. XPS study of sulfide minerals surface oxidation under high-voltage nanosecond pulses. *Miner. Eng.* **2019**, *143*, 105939.
(80) Shi, J.; Li, X.; He, G.; Zhang, L.; Li, M. Electrodeposition of high-capacitance 3D CoS/graphene nanosheets on nickel foam for high-performance aqueous asymmetric supercapacitors. *J. Mater. Chem. A* **2015**, *3* (41), 20619−20626.
(81) Yi, M.; Fisher, K.; Dance, I. The formation, reactions and structures of binary cobalt phosphide clusters [CoP]- in the gas phase. *New J. Chem.* **2001**, *25* (1), 73−82.
(82) Murphy, I. A.; Rice, P. S.; Monahan, M.; Zasada, L. B.; Miller, E. M.; Raugei, S.; Cossairt, B. M. Covalent Functionalization of Nickel Phosphide Nanocrystals with Aryl-Diazonium Salts. *Chem. Mater.* **2021**, *33* (24), 9652−9665.
(83) Wu, T.; Stone, M. L.; Shearer, M. J.; Stolt, M. J.; Guzei, I. A.; Hamers, R. J.; Lu, R.; Deng, K.; Jin, S.; Schmidt, J. R. Crystallographic Facet Dependence of the Hydrogen Evolution Reaction on CoPS: Theory and Experiments. *ACS Catal.* **2018**, *8* (2), 1143−1152.
(84) Nelson, A. E.; Sun, M.; Junaid, A. S. M. On the structure and composition of the phosphosulfide overlayer on Ni2P at hydrotreating conditions. *J. Catal.* **2006**, *241* (1), 180−188.
(85) Liu, F.; Liu, C.; Zhong, X. Enhancing electrocatalysis for hydrogen production over CoP catalyst by strain: a density functional theory study. *Phys. Chem. Chem. Phys.* **2019**, *21* (18), 9137−9140.
(86) Goldsmith, B. R.; Peters, B.; Johnson, J. K.; Gates, B. C.; Scott, S. L. Beyond Ordered Materials: Understanding Catalytic Sites on Amorphous Solids. *ACS Catal.* **2017**, *7* (11), 7543−7557.
(87) Li, K.; Wang, R.; Chen, J. Hydrodeoxygenation of Anisole over Silica-Supported Ni_2P, MoP, and NiMoP Catalysts. *Energy Fuels* **2011**, *25* (3), 854−863.
(88) Rensel, D. J.; Kim, J.; Bonita, Y.; Hicks, J. C. Investigating the multifunctional nature of bimetallic FeMoP catalysts using dehydration and hydrogenolysis reactions. *Appl. Catal. A: Gen.* **2016**, *524*, 85−93.
(89) Peroni, M.; Lee, I.; Huang, X.; Baráth, E.; Gutiérrez, O. Y.; Lercher, J. A. Deoxygenation of Palmitic Acid on Unsupported Transition-Metal Phosphides. *ACS Catal.* **2017**, *7* (9), 6331−6341.
(90) Rensel, D. J.; Kim, J.; Jain, V.; Bonita, Y.; Rai, N.; Hicks, J. C. Composition-directed $Fe_XMo_{2-X}P$ bimetallic catalysts for hydrodeoxygenation reactions. *Catal. Sci. Technol.* **2017**, *7* (9), 1857−1867.
(91) Bonita, Y.; Hicks, J. C. Periodic Trends from Metal Substitution in Bimetallic Mo-Based Phosphides for Hydrodeoxygenation and Hydrogenation Reactions. *J. Phys. Chem. C* **2018**, *122* (25), 13322−13332.
(92) Jain, V.; Bonita, Y.; Brown, A.; Taconi, A.; Hicks, J. C.; Rai, N. Mechanistic insights into hydrodeoxygenation of phenol on bimetallic phosphide catalysts. *Catal. Sci. Technol.* **2018**, *8* (16), 4083−4096.
(93) Tong, Z.; Li, X.; Dong, J.; Gao, R.; Deng, Q.; Wang, J.; Zeng, Z.; Zou, J.-J.; Deng, S. Adsorption Configuration-Determined Selective Hydrogenative Ring Opening and Ring Rearrangement of Furfural over Metal Phosphate. *ACS Catal.* **2021**, *11* (11), 6406−6415.
(94) Shi, H.; Xu, N.; Zhao, D.; Xu, B.-Q. Immobilized PVA-stabilized gold nanoparticles on silica show an unusual selectivity in the hydrogenation of cinnamaldehyde. *Catal. Commun.* **2008**, *9* (10), 1949−1954.
(95) Führer, M.; van Haasterecht, T.; Bitter, J. H. Cinnamaldehyde hydrogenation over carbon supported molybdenum and tungsten carbide catalysts. *Chem. Commun.* **2022**, *58* (98), 13608−13611.
(96) Zhu, Y.; Zaera, F. Selectivity in the catalytic hydrogenation of cinnamaldehyde promoted by Pt/SiO_2 as a function of metal nanoparticle size. *Catal. Sci. Technol.* **2014**, *4* (4), 955−962.
(97) Hájek, J.; Kumar, N.; Mäki-Arvela, P.; Salmi, T.; Murzin, D. Y.; Paseka, I.; Heikkilä, T.; Laine, E.; Laukkanen, P.; Väyrynen, J. Ruthenium-modified MCM-41 mesoporous molecular sieve and Y zeolite catalysts for selective hydrogenation of cinnamaldehyde. *Appl. Catal. A: Gen.* **2003**, *251* (2), 385−396.
(98) Fujita, S.; Nakajima, K.; Yamasaki, J.; Mizugaki, T.; Jitsukawa, K.; Mitsudome, T. Unique Catalysis of Nickel Phosphide Nanoparticles to Promote the Selective Transformation of Biofuranic Aldehydes into Diketones in Water. *ACS Catal.* **2020**, *10* (7), 4261−4267.
(99) Lee, Y.-K.; Oyama, S. T. Bifunctional nature of a SiO_2-supported Ni_2P catalyst for hydrotreating: EXAFS and FTIR studies. *J. Catal.* **2006**, *239* (2), 376−389.
(100) Carenco, S.; Portehault, D.; Boissière, C.; Mézailles, N.; Sanchez, C. Nanoscaled Metal Borides and Phosphides: Recent Developments and Perspectives. *Chem. Rev.* **2013**, *113* (10), 7981−8065.

(101) Rodriguez, J. A.; Kim, J.-Y.; Hanson, J. C.; Sawhill, S. J.; Bussell, M. E. Physical and Chemical Properties of MoP, Ni_2P, and MoNiP Hydrodesulfurization Catalysts: Time-Resolved X-ray Diffraction, Density Functional, and Hydrodesulfurization Activity Studies. *J. Phys. Chem. B* **2003**, *107* (26), 6276−6285.
(102) Sawhill, S. J.; Phillips, D. C.; Bussell, M. E. Thiophene hydrodesulfurization over supported nickel phosphide catalysts. *J. Catal.* **2003**, *215* (2), 208−219.
(103) Sun, F.; Wu, W.; Wu, Z.; Guo, J.; Wei, Z.; Yang, Y.; Jiang, Z.; Tian, F.; Li, C. Dibenzothiophene hydrodesulfurization activity and surface sites of silica-supported MoP, Ni_2P, and NiMoP catalysts. *J. Catal.* **2004**, *228* (2), 298−310.
(104) Hutchings, G. J. Promotion in Heterogeneous Catalysis: A Topic Requiring a New Approach? *Catal. Lett.* **2001**, *75* (1), 1−12.

https://doi.org/10.1021/jacs.3c07312
J. Am. Chem. Soc. 2023, 145, 23556−23567